Enhancing Joint Torque Control of Series Elastic Actuators with Physical Damping

Min Jun Kim, Alexander Werner, Florian Christoph Loeffl, and Christian Ott

***Abstract*— This paper presents that the joint torque control capability can be enhanced by adding physical damper to a series elastic actuator (SEA). Joint torque tracking of standard SEA has known limitations that the torque dynamics has an relative order of two, and, as a consequence, the torque controller often requires acceleration feedback when the desired torque is defined by a function of velocity (for example, compliance control). This limitation can be removed by introducing physical damping, reducing the relative degree of torque dynamics by one. Based on this observation, we design a robust controller using the disturbance observer technique. The resulting control law is given by a feed-forward term combined with PI control. The proposed controller is verified in simulation and experiment.**

I. Introduction

Adding physical elasticity in robot joints has impacted the robotic community for decades since being proposed in [**?**]. The intrinsic compliance of series elastic actuators (SEAs) motivated a huge number of applications such as compliant rehabilitation devices [**?**], [**?**], [**?**], human-friendly robot designs [**?**], [**?**] and robots which walk, jump, and run using energy storage provided by the elastic element [**?**], [**?**], [**?**].

One important branch of SEA research is joint torque control [**?**], [**?**], [**?**], [**?**], [**?**], [**?**], [**?**], [**?**]. Let us consider the dynamics of a SEA system ($D_j = 0$ in Fig. 1) given by

$$B\ddot{\theta} + \tau_j = \tau_m \tag{1}$$

$$M\ddot{q} = \tau_j + \tau_{ext}, \tag{2}$$

where B, M represent motor and link-side inertia, θ, q represent motor and link side position, and τ_m, τ_j, τ_{ext}, represent motor torque, joint torque, and external torque, respectively. In a typical elastic joint setup, τ_j can be observed either by sensor or system state, but τ_{ext} is usually unknown. We also would like to mention that, although this paper will mainly consider a one degree-of-freedom (DOF) formulation for simplicity, it can be easily applied to general multi-DOF robots, as will be discussed later.

To motivate the necessity of joint torque controllers, we observe that (1)-(2) form a fourth order dynamics. This makes it difficult to access the link-side dynamics from the motor torque τ_m. This is especially true when the motor-side inertia is large so that its dynamics is not negligible. Meanwhile, joint torque control enables us to directly access the link-side dynamics (Fig. 2). As a consequence, applications of SEA can be further extended as we only need to take care of link-side dynamics; i.e., any existing rigid body controller can be applied.

The authors are with Institute of Robotics and Mechatronics, German Aerospace Center (DLR), 82234 Wessling, Germany. E-mail: {minjun.kim, alexander.werner, florian.loeffl, christian.ott}@dlr.de

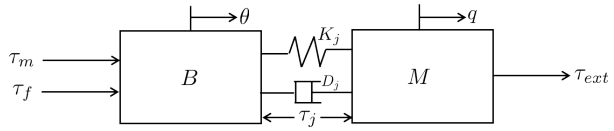

Fig. 1. Schematic diagram of a SEA system with physical joint damping D_j. This paper claims that the joint torque control capability can be enhanced by introducing D_j.

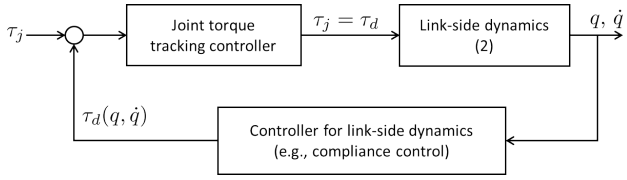

Fig. 2. Overview of the control scheme. Link-side rigid body dynamics can be controlled via joint torque tracking. τ_d represents the desired joint torque designed for the link-side rigid body dynamics.

One of the main difficulties in controlling the joint torque of SEAs is that the relative degree of torque dynamics is two.[1] Because of this, the joint torque tracking controller in Fig. 2 usually requires D-control to provide stability as well as acceptable tracking performance [**?**], [**?**], [**?**], [**?**]. However, in most of robotic applications, D-control implies feedback of $\ddot{q}$ because the desired torque is usually a function of not only q, but also $\dot{q}$. As $\ddot{q}$ should be obtained numerically, the achievable tracking performance may not be satisfactory on real hardware which has motor torque/velocity limits.

In this paper, we claim that adding physical damping in the joint enhances the joint torque control capability.[2] In fact, there have been designs that have intentional physical damping in addition to the SEA setup [**?**], [**?**]. However, the dampers were installed mainly to reduce the oscillations caused by the elastic elements rather than improving the joint torque control. Except for a few designs, in most of SEA setups, physical damping is avoided as much as possible because it may reduce the energy efficiency. For this reason, to the best of the authors' knowledge, its benefit in the control of joint torque is rarely studied.

[1] Noting that $\tau_j = K(\theta - q)$, the second derivative is needed to related τ_j to the motor input τ_m. +

[2] SEA systems are known to be robust against impact, which could be eliminated by adding a damper. However, this can be avoided by limiting the damper torque mechanically.

An important feature of physical damping is that it reduces the relative order of torque dynamics by one, as shown in [**?**]. [**?**] also showed that joint damping may increase the system bandwidth. This work, however, mainly focused on the fundamental properties of damped actuator, and did not put much effort in control aspects.[3] To complement this work, we study the fundamental differences between the classical SEA and physically damped SEA, in terms of control design. We will mainly address that the D-control is not required for physically damped SEA, so that the feedback of $\ddot{q}$ can be avoided. Based on this observation, we propose feed-forward plus PI control for the torque tracking controller which is designed using disturbance observer technique. Here, PI the gains have clear physical meanings so that we can tune the gains easily. The proposed features were verified through the simulations and experiments.

This paper is organized as follows. In section II, the limitation of the standard SEA system is reviewed and the advantage of physically damped SEA system is shown. Based on this advantage a disturbance observer control design is presented. In section III, simulation and experimental studies are shown. Section IV concludes the paper.

II. Enhancing Joint Torque Control Capability with Physical Damping

A. Limitations of standard SEA in joint torque control

A schematic diagram of standard SEA is shown in Fig. 1 (ignoring D_j). The dynamics of the overall system is given by (1)-(2) with

$$\tau_j = K_j(\theta - q). \tag{3}$$

By differentiating (3) twice, we obtain the torque dynamics:

$$\begin{aligned}\ddot{\tau}_j =& K_j(\ddot{\theta} - \ddot{q}) \\ =& K_j\left(B^{-1}(\tau_m - \tau_j) - \ddot{q})\right).\end{aligned} \tag{4}$$

Let us consider the following control law

$$\tau_m = u + \tau_j + B\ddot{q}. \tag{5}$$

Then,

$$B\ddot{\tau}_j = K_j u. \tag{6}$$

Consider the PD control law

$$u = -K_j^{-1}B\left(L_v\dot{e}_\tau + L_p e_\tau\right), \tag{7}$$

where $e_\tau = \tau_j - \tau_d$ is the torque error and τ_d is desired joint torque (see Fig. 2). Then, the closed-loop torque dynamics becomes

$$\ddot{\tau}_j + L_v\dot{e}_\tau + L_p e_\tau = 0, \tag{8}$$

or equivalently,

$$\tau_j(s) = \frac{L_v s + L_p}{s^2 + L_v s + L_p}\tau_d(s), \tag{9}$$

[3]Another difference is that the system of interest in [**?**] was series damping actuator without elasticity. In contrast, this paper is interested in series damping actuator with elasticity.

where L_v, L_p are D-, and P- control gains.

It should be noted that D-control is unavoidable here because the closed-loop dynamics (8) is unstable with $L_v = 0$. However, as D-control implies $\ddot{q}$ feedback, which will be amplified by the control gains when τ_d is a function of $\dot{q}$.[4] This is problem in the presence of noise. The following example shows the limitation of SEA torque control.

Compliance control example: We want to realize compliant behavior at a fixed position q_d, by tracking the desired torque

$$\tau_d = K_d(q_d - q) - D_d\dot{q}, \tag{10}$$

where K_d and D_d represent the desired stiffness and damping. In applying the control law (5)-(7), the most problematic term is $L_v\dot{e}_\tau = L_v(\dot{\tau}_j - \dot{\tau}_d)$ which implies $\ddot{q}$ feedback because

$$L_v\dot{\tau}_d = L_v\left(-K_d\dot{q} - D_d\ddot{q}\right). \tag{11}$$

In other words, the acceleration which is affected by noise is multiplied by $L_v D_d$, which makes the controller less robust (in fact, the derivative of τ_j is also affected by the presence of noise in a torque sensor).

B. Joint torque control of SEA with physical damping

This section shows that introducing the damping in the joint (Fig. 1) can enhance the torque controller. Now, the torque dynamics can be obtained by

$$\tau_j = K_j(\theta - q) + D_j(\dot{\theta} - \dot{q}) \tag{12}$$

$$\begin{aligned}\dot{\tau}_j =& K_j(\dot{\theta} - \dot{q}) + D_j(\ddot{\theta} - \ddot{q}) \\ =& K_j(\dot{\theta} - \dot{q}) + D_j\left(B^{-1}(-\tau_j + \tau_m) - \ddot{q})\right).\end{aligned} \tag{13}$$

Note that the relative degree of torque dynamics is one, whereas that of the SEA is two. Although we can design a torque tracking controller using (13) as will be shown in next section, let us take one more derivative to make a direct comparison with SEA.

$$\begin{aligned}&\ddot{\tau}_j = K_j(\ddot{\theta} - \ddot{q}) + D_j\left(B^{-1}(-\dot{\tau}_j + \dot{\tau}_m) - \dddot{q})\right) \\ &= K_j(B^{-1}(-\tau_j + \tau_m) - \ddot{q}) + D_j\left(B^{-1}(-\dot{\tau}_j + \dot{\tau}_m) - \dddot{q})\right).\end{aligned} \tag{14}$$

Substituting (5) into (14), we obtain

$$B\ddot{\tau}_j = D_j\dot{u} + K_j u. \tag{15}$$

It is interesting to note that D-action can be generated by P-control law.

Keeping this in mind, consider the P control

$$u = -BL_p e_\tau. \tag{16}$$

Then, the closed-loop torque dynamics becomes

$$\ddot{\tau}_j + L_p D_j\dot{e}_\tau + L_p K_j e_\tau = 0, \tag{17}$$

[4]It would be worthwhile to mention that feed-forward term $\ddot{q}$ in (5) may be less harmful because it is not amplified by any control gains.

or equivalently,

$$\tau_j(s) = \frac{L_p D_j s + L_p K_j}{s^2 + L_p D_j s + L_p K_j} \tau_d(s). \tag{18}$$

Note that the closed-loop dynamics (17) is stable without any D-control law. In other words, we can completely avoid a D-control law for physically damped SEA systems.

C. A robust control design based on disturbance observer

In previous sections, we addressed that the D-control is not required for physically damped SEA systems in terms of stability. For robust performance, we propose disturbance-observer-based control design for compensating the friction τ_f. Note that friction (or any other disturbances) is not considered so far, but the friction affects the control performance. Adding friction to the motor-side dynamics (1):

$$B\ddot{\theta} + \tau_j = \tau_m + \tau_f. \tag{19}$$

The disturbance-observer-based control law will estimate and compensate for the friction.

Because designing a robust controller is not the main goal of the paper, we leave the derivation in the Appendix. The resulting control law is given by

$$\tau_m = K_j D_j^{-1} u + \tau_j - B D_j^{-1} K_j (\dot{\theta} - \dot{q}) + B\ddot{q} \tag{20}$$

with

$$u = \dot{\tau}_d - (L_{nom} + L_{dob}) e_\tau - L_{nom} L_{dob} \int e_\tau. \tag{21}$$

Remark 1 (Physical meanings of PI gains): In the control law, L_{nom} represents the gain for nominal performance, and L_{dob} represents the gain for disturbance rejection. In principle, as $L_{dob} \to \infty$, the closed-loop dynamics becomes $\dot{e}_\tau + L_{nom} e_\tau = 0$. Please refer to Appendix for more details.

D. Discussion of the proposed controller

1) Natural velocity feedback effect: In joint torque control problems, the so-called natural velocity feedback effect plays an important role [**?**], [**?**]. This effect becomes significant when a more realistic model is assumed: the link-side dynamics is lightly damped by $D_l \dot{q}$, extending the link-side dynamics to

$$M\ddot{q} + D_l \dot{q} = \tau_j + \tau_{ext}. \tag{22}$$

Then, a zero from $(Ms + D_l)$, which is located very close to the imaginary axis, appears in the numerator of the transfer function for $\dot{\theta} \to \tau_j$. Because of this zero, joint torque control performance is significantly limited. Hence, to overcome this limitation, link-motion compensation (i.e., elimination of $\dot{q}/\ddot{q}$) in torque dynamics is very important [**?**].

One simple link-motion compensation is to directly feedforward $B\ddot{q}$ as shown in (5). This approach requires numerical calculation of $\ddot{q}$, but it has been shown that this method works in practical applications [**?**], [**?**] probably because $\ddot{q}$ is not amplified by any control gains. If numerical calculation of $\ddot{q}$ is to be avoided, an alternative is to substitute $\ddot{q}$ by $\ddot{q} = M^{-1}(\tau_j + \tau_{ext})$ from (1). One may treat τ_{ext} as disturbance if it is not known.

Even if there remains some - but small - uncompensated link motion (for example, because $D_l \dot{q}$ is hard to identify), it does not play a significant role anymore, because the closed-loop torque dynamics under (20)-(21) is

$$\dot{e}_\tau + (L_{nom} + L_{dob}) e_\tau + L_{nom} L_{dob} \frac{1}{s} e_\tau = -\alpha \dot{q}, \tag{23}$$

where α is a small value that represents the uncompensated link motion. Using $\dot{q}(s) = \frac{1}{Ms + D_l} \tau_j(s)$ (τ_{ext}-related term is neglected because this is irrelevant to the analysis) and $e_\tau = \tau_j - \tau_d$, we obtain

$$\tau_j(s) = \frac{(s + L_p + L_i \frac{1}{s})(Ms + D_l)}{(s + K_p + L_i \frac{1}{s})(Ms + D_l) + \alpha} \tau_d(s), \tag{24}$$

where $L_p = L_{nom} + L_{dob}$ and $L_i = L_{nom} L_{dob}$. Because $(s + L_p + L_i \frac{1}{s})(Ms + D_l) \gg \alpha$, a pole, which is located very close to $-D_l/M$, virtually cancels the effect of zero.

The important point is that, whatever approach we use, the link-motion should be reasonably compensated in order to avoid natural velocity feedback effect that limits joint torque control performance.

2) Extension to multi-DOF robots: So far, the formulation is presented for the single-DOF case. However, it can be generalized by a few modifications. The dynamics for the multi-DOF is given by

$$B\ddot{\theta} + \tau_j = \tau_m + \tau_f \tag{25}$$

$$M(q)\ddot{q} + C(q, \dot{q})\dot{q} + g(q) = \tau_j + \tau_{ext}, \tag{26}$$

$$\tau_j = K_j(\theta - q) + D_j(\dot{\theta} - \dot{q}) \tag{27}$$

where parameters are now matrix/vector valued quantities.

Torque dynamics can then be described by

$$\dot{\tau}_j = K_j(\dot{\theta} - \dot{q}) + D_j \left(B^{-1}(-\tau_j + \tau_m) - \ddot{q} \right), \tag{28}$$

which is identical to (13). The rest of control design can be done in the same way.

3) Zero dynamics: As one can see in (1)-(2), the overall system dynamics is fourth order. However, in controlling these, we only considered the first order torque dynamics (more precisely, relative degree of one). The remaining third order is the zero dynamics that cannot be accessed anymore.

Namely, in addition to the state τ_j, there are three more states in describing the overall dynamics. Two states are link-side position and velocity q, $\dot{q}$ governed by (2). Noting that the joint torque τ_j converges to τ_d exponentially and, assuming that τ_d is designed properly, these two states are stable. Another state is $\delta = \theta - q$ which is governed by $K_j \delta + D_j \dot{\delta} = \tau_j$. Again, because τ_j exponentially converges to τ_d, δ remains finite.

In conclusion, in controlling the overall fourth order dynamics, it is sufficient to control the first order torque dynamics together with stabilizing control law τ_d for the link-body dynamics.

TABLE I

SYSTEM PARAMETERS USED IN THE SIMULATION

Description	Symbol	Value
Motor side Inertia	B	$1.62\ \mathrm{kg \cdot m^2/s^2}$
Link side Inertia	M	$0.5\ \mathrm{kg \cdot m^2/s^2}$
Joint stiffness	K_j	$500\ \mathrm{Nm/rad}$
End stop stiffness	·	$10000\ \mathrm{Nm/rad}$
End stop damping	·	$10\ \mathrm{Nm \cdot s/rad}$
Joint damping	D_j	100 (0 for standard SEA) $\mathrm{Nm \cdot s/rad}$
Link-side damping	D_l	$0.01\ \mathrm{Nm \cdot s/rad}$
Friction	τ_f	emulates harmonic drive friction
Motor saturation	·	$\pm 100\ \mathrm{Nm}$

III. SIMULATION AND EXPERIMENTS

In this section, simulations and experiments are shown to compare the torque control capabilities of standard SEA and the physically damped SEA systems. The parameters used in the simulations are summarized in Table I. Note that the motor torque is saturated at ± 100, and $D_l\dot{q}$ which may cause natural velocity feedback effect (discussed in Section II-D) is considered to be unknown.

A. Torque control for SEA

The disturbance-observer-based control design presented for physically damped SEA (see Appendix) can be applied to the standard SEA systems. One difference is that the standard SEA system has the second order torque dynamics (5). Hence, for (5), we use the following control law:

$$\tau_m = BK_j^{-1}(u + u_{dob}) + \tau_j + B\ddot{q} \tag{29}$$

with

$$u + u_{dob} = \ddot{\tau}_d - (L_{nom,v} + L_{dob})\dot{e}_\tau - (L_{dob}L_{nom,v} + L_{nom,p})e_\tau - L_{dob}L_{nom,p}\int e_\tau. \tag{30}$$

Similar to Remark 1, $L_{dob,v}$, $L_{dob,p}$ determine the nominal performance, and L_{dob} determines the disturbance rejection performance. In fact, similar PID (or PD)+feedforward control is commonly used in SEA literature; e.g. [**?**], [**?**].

B. Scenario for Experiments and Simulations

In the simulations and experiments, the following compliance control with gravity compensation (recall the example presented in Section II-A) was used:

$$\tau_d = K_d(q_d - q) - D_d\dot{q} + g(q_d). \tag{31}$$

The control gains used in the simulations and experiments are summarized in Table II. Note that the maximum D_d that could be achieved in the SEA experiment was lower than that of physically damped SEA experiment. The reason will be explained shortly.

Experiments were performed as follows for both SEA and physically damped SEA:

1) At the beginning, the initial position was $q \simeq 0$, and the desired position was set as $q_d = -\pi/12$.
2) While staying at $q \simeq -\pi/12$, a human operator applied external torque to observe if the compliance behavior is realized.
3) The desired position was suddenly changed to $q_d = \pi/12$ which the link cannot reach due to the end stop (i.e., a collision occurs).
4) While staying at $q \simeq 0$ (desired is $q_d = \pi/12$, but cannot reach due to the end stop), human applied external torque to see if the compliance behavior is realized.

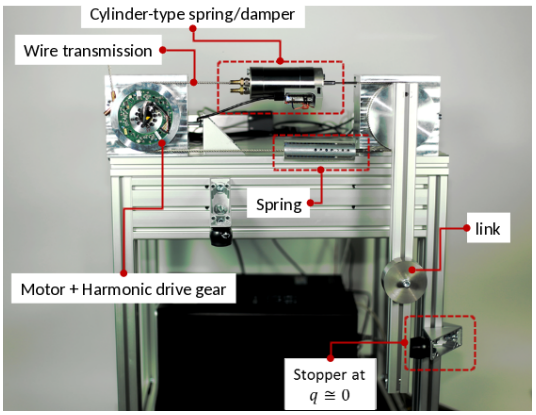

Fig. 3. Experimental setup. The left disc (motor-side) is connected by steel cables to the right disc (link-side). A joint of DLR LWR is used for the motor module (with 1:100 gear ratio). The upper element generates viscous damping (to be precise, cylinder also has some amount of stiffness), and the lower element contains steel spring. An end-stop is located near $q = 0$ which is used as a wall in the experiments. The SEA setup was realized by replacing cylinder-type spring-damper element by a spring element.

Simulations were performed for 3)-4) in the above scenario, but without human interaction. Note that the collision part is involved because it induces large $\ddot{q}$. In simulations, end stop was modeled as spring damper (see Table. I). In addition, the result of ideal torque source case (i.e., the $\tau_j \equiv \tau_d$) is also provided for comparison.

C. Simulation

1) SEA: Two sets of gains (high and low gains in Table II) were used in the SEA simulation to show the trade-off between torque tracking performance and interaction robustness.

It is obvious that the high gain setup has better torque tracking performance, as shown in Fig. 4. However, high control gains did not stabilize the system when there was a collision with environment. Note that the acceleration signal is amplified by $D_d(L_{nom,v} + L_{dob})$ (where $(L_{nom,v} + L_{dob})$ is the D-gain of the torque tracking controller), the motor torque quickly hits the saturation (Fig. 5a). As a result, the torque tracking was not good (Fig. 5b), and the resulting motion was far from ideal (Fig.6).

When it comes to real world, the controlled system was vulnerable under disturbances caused by various sources (e.g., time delays, quantization error, sensor noise), so it easily became unstable.

TABLE II

CONTROL PARAMETERS USED IN THE EXPERIMENTS AND SIMULATIONS

Description	Symbol	Value
Experiment and simulation of physically damped SEA	L_{nom}	10
	L_{dob}	1000
	K_d	100
	D_d	20
Experiment and simulation of standard SEA	$L_{nom,v}$	10
	$L_{nom,p}$	25
	L_{dob}	simulation (high gain): 1000 simulation (low gain): 50 experiment: 50
	K_d	100
	D_d	simulation (high gain): 20 simulation (low gain): 5 experiment: 5

Using the low gains (note that both D_d and L_{dob} were lowered to reduce the acceleration feedback[5]), despite worse tracking performance, the controlled system was more robust against collision. As shown in Fig. 7a, the motor torque was not saturated. Although the torque tracking performance was not satisfactory (Fig. 7b), the resulting link-motion was closer to the ideal (Fig. 6).

In conclusion, for SEA systems, it was difficult to achieve robustness against collision while maintaining torque tracking performance. One big reason for this is the acceleration feedback which is amplified not only by the D-control gain of the inner-loop torque tracking controller, but also by the damping value of the outer-loop compliance controller. In the experiments, the low gains were used for this reason.

2) Physically damped SEA: Because the torque control of physically damped SEA does not require D control law which implies acceleration feedback, we can achieve robustness against collision without sacrificing the torque tracking performance. Even though the high gains ($L_{dob} = 1000$) were used, the control input was not saturated except for short instants (Fig. 8). As a result, the torque tracking was reasonable and the resulting link-motion was close to the ideal case (Fig. 6).

D. Experiments

1) SEA: As discussed in the simulation section, low control gains were used (experiment failed with high control gains). Although the resulting motion q, q_d in Fig. 9a looks reasonable, low level torque tracking (Fig. 9b) was not satisfactory when the collision occurred (Fig. 9c). In addition, because of the heavy noise imposed by the calculation of $\ddot{q}$, the controlled system suffered from the chattering, even without the collision (Fig. 10).

2) Physically damped SEA: Although the high control gain ($L_{dob} = 1000$) was used, both the torque tracking and resulting link-motion were reasonable (Fig. 11). In addition, the resulting control input was free of chattering because the resulting control did not require D-control.

[5]When we reduced only L_{dob} without changing D_d, the tracking performance was not acceptable.

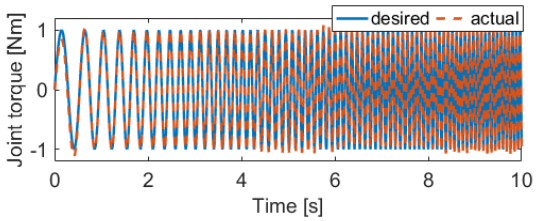

(a) Torque tracking of standard SEA with $L_{dob} = 1000$

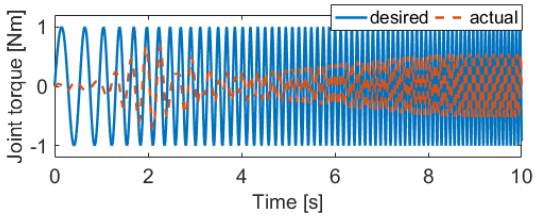

(b) Torque tracking of standard SEA with $L_{dob} = 50$

Fig. 4. Torque tracking for test signal (chirp signal of 2Hz to 8Hz) (a) with high gain and (b) with low gain.

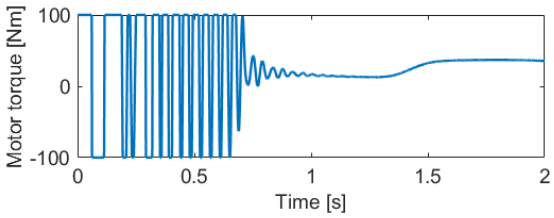

(a) Applied motor input

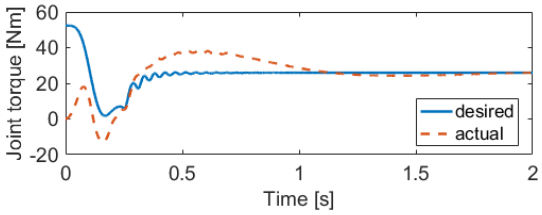

(b) Joint torque tracking

Fig. 5. Simulation results for SEA with high gain setting. (a) Control input easily hits the maximum value (saturation) due to the noisy $\ddot{q}$ feedback. (b) As a result, the joint torque tracking was not successful.

IV. CONCLUSION

In this paper, it is shown that the physical joint damping enhances the joint torque tracking capability of SEA, mainly because it reduces the relative degree of torque dynamics order by one. Unlike the damping-free SEA (i.e. standard SEA) case, physically damped SEA is stable without D-control. This may significantly enhance the joint torque tracking capability, because the D-control law often implies $\ddot{q}$ feedback which will be amplified by the D-control gain of the torque tracking controller (and also by the D-gain of the outer-loop rigid-body controller). A robust control design was proposed based on the disturbance observer technique, and the proposed scheme was verified through simulations and experiments. The standard SEA control suffered from trade-off between torque tracking performance (requiring high gain) and the robustness against collision (requiring low

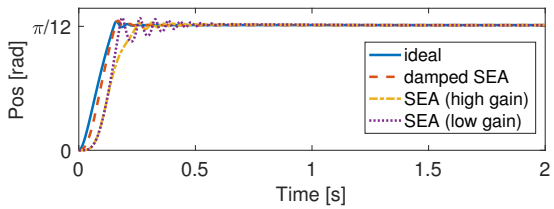

(a) Link-side behavior

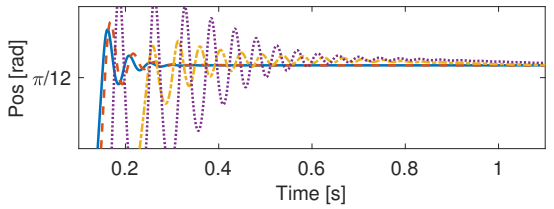

(b) Magnified view

Fig. 6. Link-side behaviors (q) of ideal torque source, standard SEA, physically damped SEA cases. Standard SEA suffered from serious bounds on the wall resulted from the imprecise torque tracking, whereas the physically damped SEA showed similar behavior to the ideal.

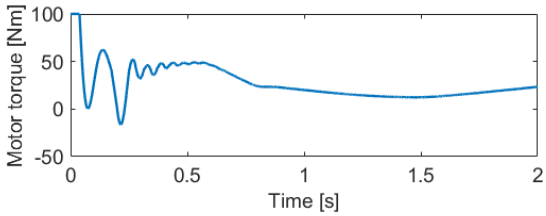

(a) Applied motor input

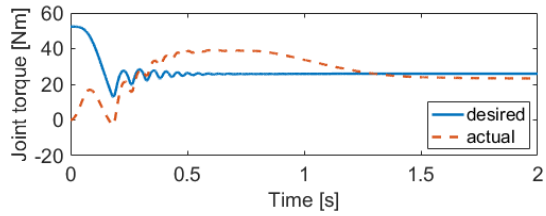

(b) Joint torque tracking

Fig. 7. Simulation results for the SEA with low gain setting. (a) Control input is not saturated, but (b) the resulting joint torque does not follow the desired torque.

gain), whereas the physically damped SEA did not suffer from this. In addition, chattering, which was observed for SEA because of the acceleration feedback, was not observed for the physically damped SEA.

APPENDIX

This Appendix shows the derivation of the control law (20)-(21) based on disturbance observer technique.

Substituting (20) into (13), we have

$$\dot{\tau}_j = u + u_{dob} + \underbrace{w}_{=DB^{-1}\tau_f}, \tag{32}$$

where w is the disturbance. Defining $u = \dot{\tau}_d - L_{nom}e_\tau$, the closed-loop torque dynamics becomes

$$\dot{e}_\tau + L_{nom}e_\tau = u_{dob} + w, \tag{33}$$

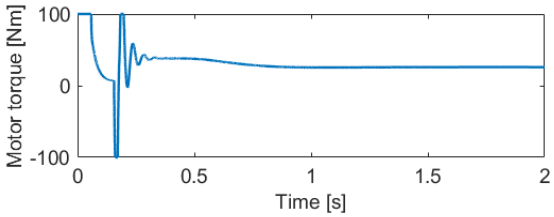

(a) Applied motor input

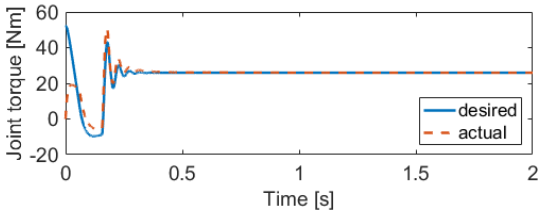

(b) Joint torque tracking

Fig. 8. Simulation results for the physically damped SEA. (a) Control input was not saturated except for some short instants even with the high control gains. (b) As a result, the joint torque tracking showed better result than the standard SEA case.

Hence, If u_{dob} can estimate and compensate for w (i.e., $u_{dob} \simeq -w$), then the exponential tracking can be achieved.

To this end, define the observer dynamics by

$$\dot{\hat{\tau}}_j = u. \tag{34}$$

Finally, define u_{dob} by

$$u_{dob} = L_{dob}(\hat{\tau}_j - \tau_j). \tag{35}$$

It should be noted that u_{dob} estimates w because

$$\begin{aligned} u_{dob} =& L_{dob}(\hat{\tau}_j - \tau_j) && (36)\\ =& L_{dob}\left(\frac{1}{s}u - \frac{1}{s}(u_{dob} + u + w)\right). && (37)\end{aligned}$$

After simple algebraic manipulation,

$$u_{dob} = -\frac{L_{dob}}{s + L_{dob}}w. \tag{38}$$

The resulting $u+u_{dob}$ is nothing but the feed-forward plus PI controller because

$$\begin{aligned} u + u_{dob} =& \dot{\tau}_d - L_{nom}(\tau_j - \tau_d) + L_{dob}(\hat{\tau}_j - \tau_j)\\ =& \dot{\tau}_d - L_{nom}(\tau_j - \tau_d) + L_{dob}(\int u - \tau_j)\\ =& \dot{\tau}_d - (L_{nom} + L_{dob})e_\tau - L_{nom}L_{dob}\int e_\tau. \end{aligned} \tag{39}$$

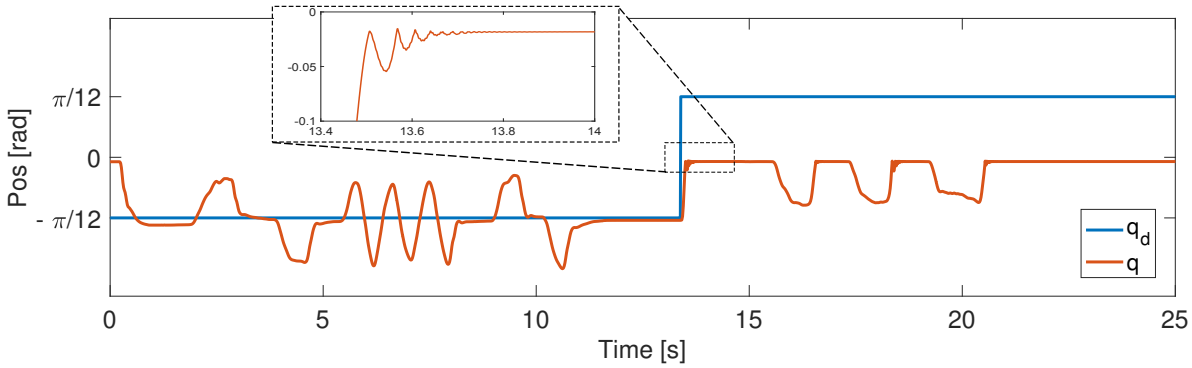

(a) Link-side behavior

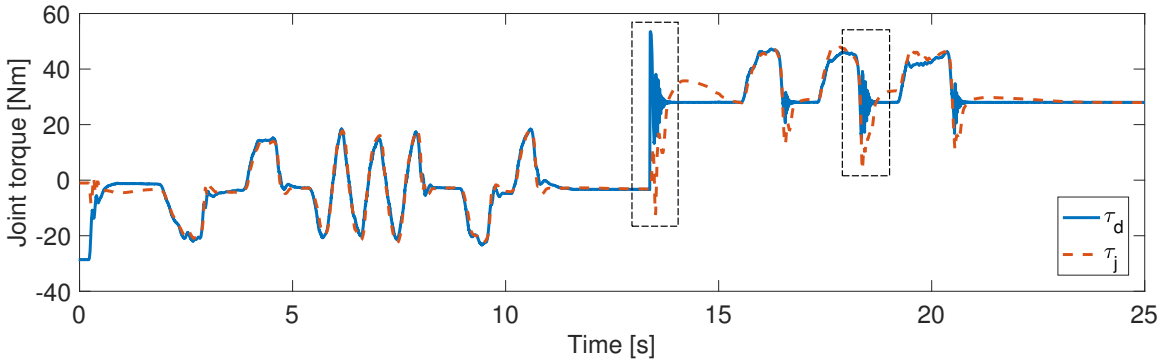

(b) Torque tracking performance

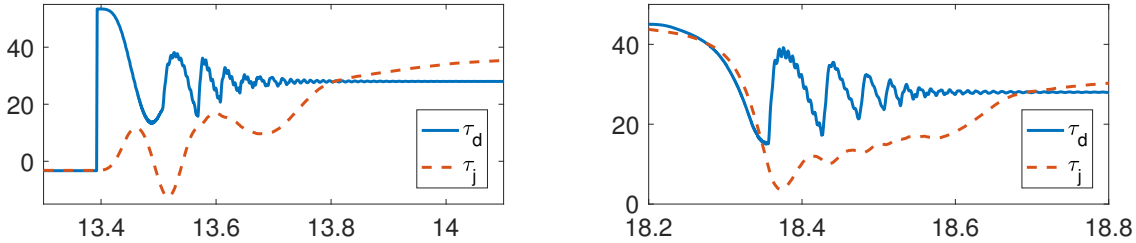

(c) Magnified view for black dashed box in (b)

Fig. 9. Experimental results for SEA. Initially, desired position of the compliance controller was $-\pi/12$, and changed to $\pi/12$. There was a collision near $q = 0$ due to the end stop. During the operation, human keep applied external torque.

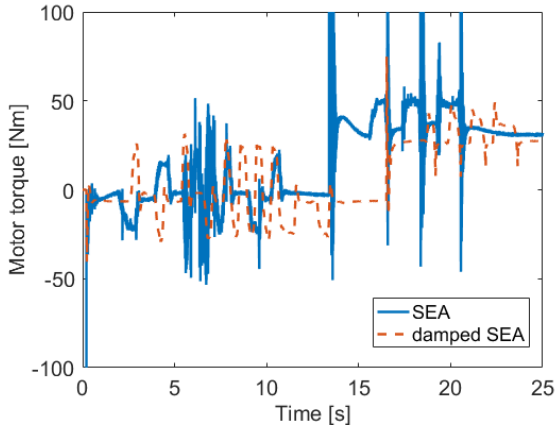

Fig. 10. Applied motor input. SEA torque control suffered from chattering because of acceleration feedback, whereas physically damped SEA control was not.

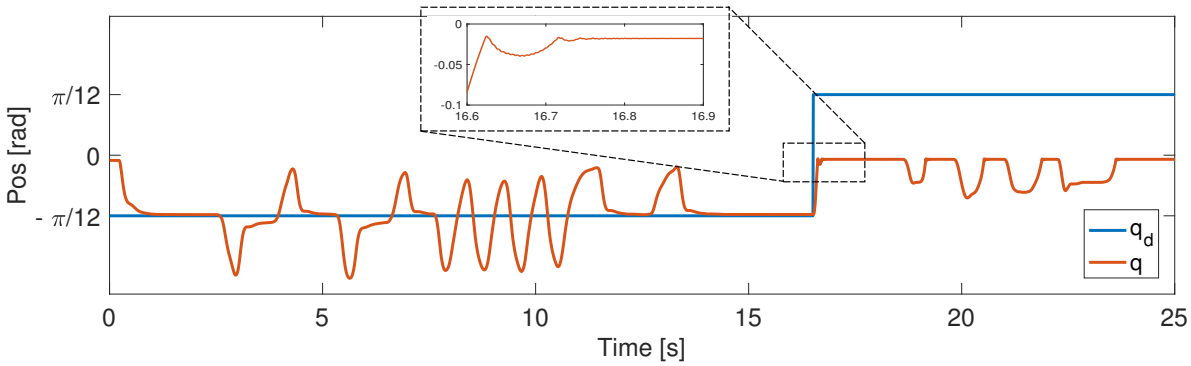

(a) Link-side behavior

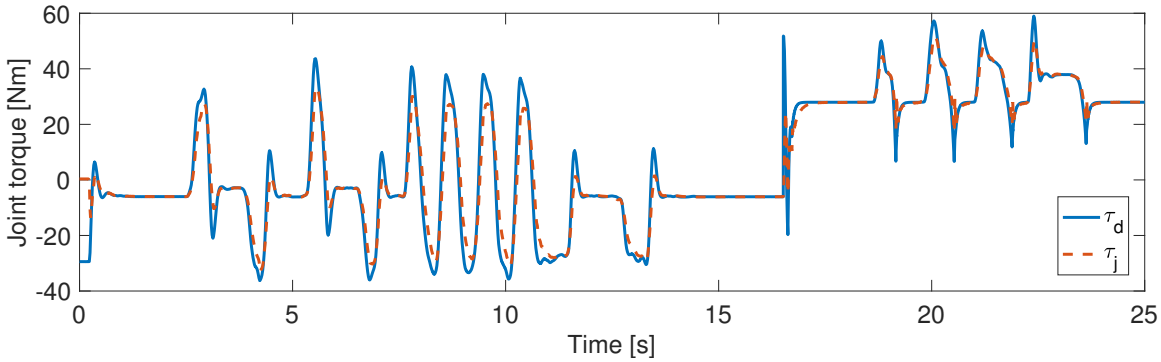

(b) Torque tracking performance

Fig. 11. Experimental results for physically damped SEA. Initially, desired position of the compliance controller was $-\pi/12$, and changed to $\pi/12$. There was a collision near $q = 0$ due to the end stop. During the operation, human keep applied external torque.